Co-processing of raw and washed air pollution control residues from energy-from-waste facilities in the cement kiln

Bogush, A., Stegemann, J., Zhou, Q., Wang, Z., Zhang, B., Zhang, T., Zhang, W. & Wei, J.

Original citation & hyperlink:
Bogush, A, Stegemann, J, Zhou, Q, Wang, Z, Zhang, B, Zhang, T, Zhang, W & Wei, J 2020, 'Co-processing of raw and washed air pollution control residues from energy-from-waste facilities in the cement kiln' Journal of Cleaner Production, vol. 254, 119924. https://dx.doi.org/10.1016/j.jclepro.2019.119924

DOI 10.1016/j.jclepro.2019.119924
ISSN 0959-6526
ESSN 1879-1786

Publisher: Elsevier

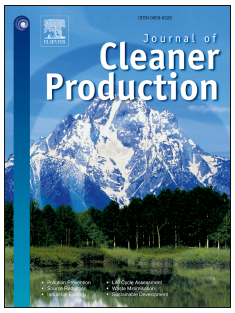

Co-processing of raw and washed air pollution control residues from energy-from-waste facilities in the cement kiln

Anna A. Bogush, Julia A. Stegemann, Qizhi Zhou, Zhiyong Wang, Bin Zhang, Tongsheng Zhang, Wensheng Zhang, Jiangxiong Wei

PII: S0959-6526(19)34794-8

DOI: https://doi.org/10.1016/j.jclepro.2019.119924

Reference: JCLP 119924

To appear in: *Journal of Cleaner Production*

Received Date: 7 February 2019

Revised Date: 22 December 2019

Accepted Date: 29 December 2019

Please cite this article as: Bogush AA, Stegemann JA, Zhou Q, Wang Z, Zhang B, Zhang T, Zhang W, Wei J, Co-processing of raw and washed air pollution control residues from energy-from-waste facilities in the cement kiln, *Journal of Cleaner Production* (2020), doi: https://doi.org/10.1016/j.jclepro.2019.119924.

Co-processing of Raw and Washed Air Pollution Control Residues from Energy-from-Waste Facilities in the Cement Kiln

CRediT author statement

Anna A. Bogush: Methodology, Investigation, Formal Analysis, Writing-Original Draft, Visualisation; **Julia A. Stegemann:** Conceptualisation, Methodology, Formal Analysis, Writing-Original Draft, Writing-Review & Editing, Supervision, Project Administration, Funding Acquisition; **Qizhi Zhou:** Investigation; **Zhiyong Wang:** Investigation; **Bin Zhang:** Investigation; **Tongsheng Zhang:** Methodology, Writing-Review & Editing, Supervision; **Wensheng Zhang:** Conceptualisation, Methodology, Resources, Supervision, Project Administration, Funding Acquisition; **Jiangxiong Wei:** Methodology, Resources, Supervision, Project Administration, Funding Acquisition.

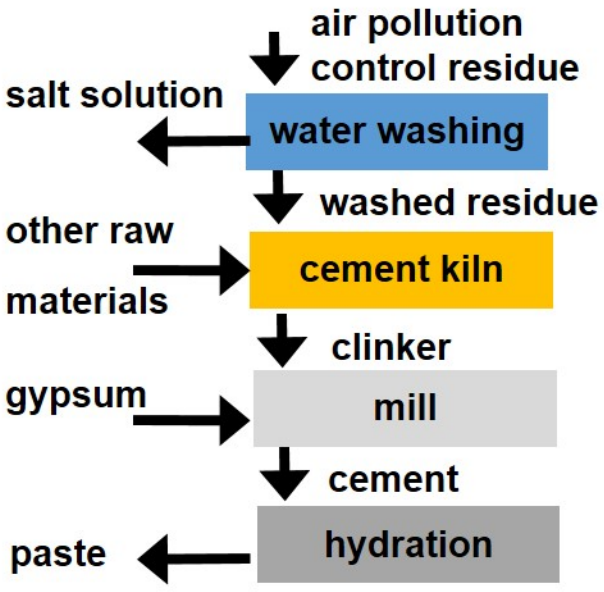
air pollution
control residue
salt solution
water washing
washed residue
other raw
materials
cement kiln
clinker
gypsum
mill
cement
paste
hydration

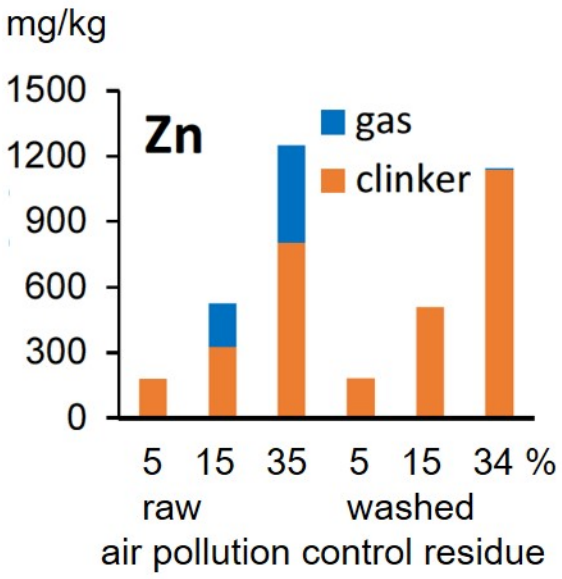
mg/kg
1500
1200
900
600
300
0
Zn
gas
clinker
5 15 35 5 15 34 %
raw
washed
air pollution control residue

Co-processing of Raw and Washed Air Pollution Control Residues from Energy-from-Waste Facilities in the Cement Kiln

Anna A. Bogush[a], **Julia A. Stegemann[a*]**, Qizhi Zhou[a], Zhiyong Wang[b], Bin Zhang[c], Tongsheng Zhang[c], Wensheng Zhang[b], Jiangxiong Wei[c]

[a]Centre for Resource Efficiency & the Environment (CREE), Department of Civil, Environmental & Geomatic Engineering (CEGE), UCL, Chadwick Building, Gower Street, London, WC1E 6BT, UK

[b]The State Key Laboratory of Green Building Materials, China Building Materials Academy (CBMA), Beijing, China

[c]School of Materials Science and Engineering, South China University of Technology, Guangzhou, China

***Corresponding Author: phone: +44(0)207 679 7370; email: j.stegemann@ucl.ac.uk**

ABSTRACT: Co-processing of industrial wastes as alternative raw materials in cement manufacture is an example of industrial symbiosis for improved material resource efficiency. Since co-processing introduces impurities from wastes, such as air pollution control residue (APCR) from municipal solid waste combustion, into the cement kiln, a better understanding of their environmental impacts and effects on cement manufacturing and quality is needed. Portland cement clinkers containing 5-35% raw or 5-34% washed APCR were prepared, with formation of all typical minerals, but with effects on clinkering reactions, and increased $2CaO \cdot SiO_2$ and decreased $3CaO \cdot SiO_2$ and $3CaO \cdot Al_2O_3$. Raw APCR affected the shape of the $2CaO \cdot SiO_2$ and $3CaO \cdot SiO_2$ grains, and cement paste from clinker made with 35% APCR exhibited negligible 28d strength. Pastes from the clinkers with lower contents of APCR or washed APCR had strengths that were lower than that of the control at 7d, similar at 28d (~90 MPa) and higher at 6m (up to 120 MPa), consistent with their $2CaO \cdot SiO_2$ and $3CaO \cdot SiO_2$ contents. Utilization of minerals in APCR thus comes with a trade-off against cement quality. Volatilization of S, Cl, Pb was reduced by washing, which fully eliminated volatilization of Zn. Zn was found mainly in the interstitial phases of the clinker, in solid solution in $4CaO \cdot Al_2O_3 \cdot Fe_2O_3$ or $3CaO \cdot Al_2O_3$. Further investigation is required to determine whether Zn and other incorporated elements may be released from the cement paste when these phases react with water. APCR co-processing may reduce CO_2 emissions by avoiding $CaCO_3$ decomposition, but this is an uncertain benefit, which may be outweighed by the detrimental effects of APCR alkalis, Cl, S and metals on cement production and quality. Life cycle environmental impacts associated with washing, and dispersal of contaminants in the built environment through construction materials, are additional concerns.

KEYWORDS: incineration, waste-to-energy, fly ash, element speciation, industrial symbiosis

WORD COUNT: 7690 words

ABBREVIATIONS

AM, alumina modulus; APCR, air pollution control residue; ARM, alternative raw material; BEI, backscattered electron imaging; C_2S, belite; C_3S, alite; C_3A, aluminate; C_4AF, ferrite; EDS, energy dispersive spectroscopy; EfW, energy from waste; DSC, differential scanning calorimetry; DTG, differential thermogravimetry; HM, hydration modulus; LSF, lime saturation factor; SEI, secondary electron imaging; SEM, scanning electron microscope; SM, silica modulus; STA, simultaneous thermal analysis; TG, thermogravimetry; w-APCR, washed air pollution control residue; XRD, X-ray powder diffraction; XRF, X-ray fluorescence

INTRODUCTION

Co-processing of industrial wastes as alternative raw materials (ARM) in the cement kiln (WBCSD 2014) can be an example of eco-friendly industrial production (e.g., Nidheesh and Kumar 2019). While this practice can improve material resource efficiency, most wastes contain contaminants. Cleaner production through co-processing therefore requires a good understanding of the impacts of these contaminants on the cement manufacturing process, cement quality, and the environment (Stegemann 2014). The air pollution control residue (APCR) that arises from combustion of municipal solid waste to generate energy-from-waste (EfW) is an example of a candidate waste for co-processing. APCR arises in the flue gas cleaning process and includes fly ash and solids captured downstream from the acid gas treatment units and before the gases are released into the atmosphere. It is alkaline (corrosive) and contains high concentrations of potential pollutants and soluble anions, which is a combination that poses problems for land disposal, treatment or recovery (e.g., Gomes et al. 2016), and has resulted in its classification as hazardous waste in most jurisdictions (e.g., Chandler et al. 1997; Bogush et al. 2015). Since APCR arisings are expected to increase with increasing numbers of municipal waste incinerators and EfW plants (Lederer et al. 2017a), it is essential to develop an acceptable APCR management strategy.

Attempted APCR treatments reported in the literature include separation processes (e.g., Quina et al. 2018), blending with cement (stabilization/solidification) before landfill or utilization in construction (Stegemann 2014), and thermal methods. Thermal techniques, including vitrification, melting and sintering (Astrup et al. 2008), e.g., to produce glass (Wexell 2005), ceramics (Amutha Rani et al. 2008) and lightweight aggregates (Quina et al. 2014), have been investigated for treatment and disposal or utilization of APCR. Though offering the potential to

destroy organic pollutants (e.g., dioxins and furans) and recover toxic elements, or respeciate them in less mobile forms, the energy costs for these processes are high (Quina et al. 2008).

Co-processing of APCR in a cement kiln is a potential thermal treatment and recycling option without substantial additional energy costs. The presence of high, though variable, amounts of Ca (e.g., 22-32%, present as $CaCO_3$, $CaSO_4$, $Ca(OH)_2$, CaO and CaOHCl), as well as Si and Al (Bogush et al. 2015), in APCR suggests that it may be suitable as an ARM. It has been suggested that co-processing APCR takes advantage of the excess lime from scrubbing acid gases to avoid non-fuel CO_2 emissions from lime calcination (Ferreira et al. 2003). On the other hand, high amounts of Cl (e.g., 7-22%, present as CaOHCl, KCl and NaCl), S (e.g., 1-1.4% SO_4^{2-}), alkalis (e.g., 0.9-3.5% K and 1.2-3.5% Na) and toxic metals (e.g., 0.05-0.20% Pb and 0.26-0.73% Zn) (Bogush et al., 2015) are present as undesirable contaminants. Pretreatment of APCR by water washing can be used to reduce the content of soluble salts before blending it with other raw meal components, but does not substantially remove toxic metals (Bogush et al. 2019), and their fate in the kiln is a concern.

Previous laboratory studies of APCR co-processing have investigated the effect of raw mix composition on: formation of the required mineral phases for Portland cement, $3CaO \cdot SiO_2$, $2CaO \cdot SiO_2$, $3CaO \cdot Al_2O_3$, and $4CaO \cdot Al_2O_3 \cdot Fe_2O_3$ (C_3S, C_2S, C_3A and C_4AF in cement chemist's notation; also known as alite, belite, aluminate and ferrite); occurence of free lime, f-CaO, i.e., that did not react to form the desired calcium silicates (Shi et al. 2004; Saikia et al. 2007; Pan et al. 2008; Ma et al. 2009; Lam et al. 2011; Wang et al. 2010; Lin et al. 2015); volatilisation of alkalis and metals (Saikia et al. 2007, Wang et al. 2010); and strength of cement paste made using the resulting clinkers (Shi et al. 2004; Pan et al. 2008; Ma et al. 2009; Wang et al. 2010;

Lin et al. 2015). Other aspects not of direct relevance to the present work are reviewed in a separate paper (Stegemann et al., unpublished).

The APCR content in the previous laboratory experiments ranged from 2-50% raw APCR or 1-48% washed APCR (w-APCR), of the dry mass of the raw mix, resulting in ranges of clinker lime saturation factors (LSFs) ranging from 0.86-1.69, silica moduli (SMs) from 0.89-2.97, and alumina moduli (AMs) from 1.29-6.72. These ranges are much wider than those typical of raw mixes for Portland cements, i.e., LSF 0.92-0.98, SM 2.0-3.0, and AM 1.0-4.0 (Taylor, 1997).

The ranges of variables investigated among the previous studies was sufficiently diverse that it is difficult to generalize about the results, but it seems clear that APCR addition, whether or not it was washed, had a detrimental effect on formation of Portland cement phases. Despite lowering the temperature for formation of the liquid phase, as a result of the presence of heavy metals and action of salts as mineralizers (Shi 2004), APCR addition suppressed formation of C_3S, even in mixes with a high LSF (Saikia et al., 2007; Lam et al. 2011). Portland cement phases, with low f-CaO, could nevertheless be formed with up to 50% APCR or 45.6% w-APCR by balancing the raw mixes (Saikia et al. 2007), and the clinker phase composition was improved by washing the APCR, over the range from 2-8% addition (Lam et al. 2011). Addition of 1% w-APCR in a full-scale plant was found to have no impact on the clinker phase composition (Wang et al. 2010). With some variation between the laboratories, volatilisation was found to be nearly complete for Na, K, Pb and Cd, and significant for Zn, Cu and Cr. Volatilisation of both alkalis and metals was reduced by APCR washing, but remained substantial for Pb and Cd, and significant for Zn and Cr (Saikia et al. 2007, Wang et al. 2010). Although co-processing of very low proportions of APCR (e.g., 1%, Wang et al. 2010, or 1.75%, Pan et al. 2008) only slightly affects the strength

of cement made with the resulting clinker, cement strength was found to decline with increasing content of both APCR (Shi et al. 2004; Ma et al. 2009) and w-APCR (Lin et al. 2015).

Although these previous authors have tended to come to positive conclusions about the advisability of APCR co-processing, the effects on kiln processing and cement quality can be seen to be generally detrimental. Material and substance flow analyses have also shown that utilization of waste (Achternbosch et al., 2005), such as APCR (Lederer et al., 2017b), in construction materials has the potential to cause unacceptable increases in cement metal concentrations, but the understanding of the environmental mobility of toxic metals in clinker is poor. The present work is part of a larger project to conduct a rigorous investigation of the fate and behaviour of toxic metals from untreated wastes, through the cement kiln, clinker, and stack emissions, to hydrated cement pastes and the environment, with the overall aim of assessing whether co-processing of wastes such as APCR can be considered to be cleaner production. The understanding gained in the previous studies in the literature was used to design raw mixes with balanced compositions that would produce the best quality Portland cement clinkers possible under the constraint of APCR addition, suitable for further work to investigate metal mobility (e.g., Karakas et al. 2019; Marchand et al. 2019; Solpuker et al. 2019 and others in preparation). In addition to systematically verifying the formation of the required Portland cement phases, and conducting mass balances for Cl, S, Pb and Zn, the novel objectives addressed here were:

1) to conduct a rigorous and systematic direct comparison of the effects of co-processing APCR and w-APCR on a) thermal processing of a balanced raw mix, b) clinker formation, and c) the ability of cements made from the clinkers to gain strength when hydrated;

2) to examine the speciation of Zn, as one the main contaminants of concern in APCR, in the clinker; and

3) to estimate the quantitative impacts of APCR co-processing on CO_2 emissions.

MATERIALS AND METHODS

Materials. An approximately 10 kg composite sample of an APCR was obtained from a full-scale EfW facility at a single sampling time by the facility operator. Representative subsamples of the required size for the analyses were obtained by coning and quartering. A subsample of APCR was washed in distilled water at a liquid-to-solid ratio of 10, and air dried to constant mass at 25±3^{o}C, to prepare a sample of w-APCR. Both the APCR and w-APCR from the same facility were characterized in detail in previous work (Bogush et al. 2019). Oxide concentrations of the clinker-forming elements and alkalis measured by X-ray fluorescence (XRF), and chloride and sulphate concentrations measured by ion chromatography of a 100:1 water extract, for the specific APCR and w-APCR samples used in the current work, are shown in Table 1.

Table 1. Oxide compositions, and chloride and sulphate contents of raw and washed energy-from-waste air pollution control residues (%)

	APCR	w-APCR
CaO	47	46
MgO	1.3	1.7
SiO_2	7.9	11
Al_2O_3	8.3	10
Fe_2O_3	2.2	3.4
Na_2O	3.2	1.9
K_2O	2.5	0.89
P_2O_5	1.7	2.5
Cl^-	7.2	0.51
SO_4^{2-}	3.9	6.9

Cement clinker was prepared using three different levels of APCR or w-APCR with analytical grade pure chemical compounds, $CaCO_3$, SiO_2, Al_2O_3, and Fe_2O_3. Raw mix proportions were calculated to yield a Bogue phase composition typical of Portland cement clinker (50−70% C_3S,

15−30% C_2S, 5−10% C_3A, and 5−15% C_4AF, dry mass basis), by control of the LSFs at 0.91-0.94, the SMs at 2.44-2.86, and the AMs at 1.60-1.67 (Taylor 1997; Table 2). Mg was neglected in the calculation, as it represented <2% of the APCR. Based on these calculations, the maximum proportions of APCR and w-APCR that could be incorporated in clinker were 35% and 34%, respectively.

The raw materials were finely ground in a ball mill such that 90±2% passed an 80 µm sieve, and thoroughly homogenized in a mechanical planetary mixer. 200 g of each raw mix formulation was mixed with 8-10% of water and then compressed into a 13 cm diameter x 1 cm high disc. The discs were dried in an oven at 105°C for 1 hour before clinkering in the laboratory of the China Building Materials Academy using a high-temperature electrical furnace. The discs were calcined at 900°C for 30 min, then heated up to 1450°C at a heating rate of 20°C/min and maintained at 1450°C for 2 h. The clinkers were cooled quickly to room temperature using a blow dryer, and then smashed and finely ground in a ball mill such that 90±2% passed a 45 µm sieve.

Cement powders were produced from the ground clinkers by mixing them with 5% gypsum to control the setting time. Cement pastes with a water-to-cement ratio of 0.35 were prepared from each powder and used to make 2.5x2.5x2.5 cm^3 cube specimens, which were cured at 25±3^oC in sealed plastic bags, in the presence of a moist tissue. Unconfined compressive strengths of the cubes were measured in triplicate after 3, 7, 28 and 199 days (BS EN 12390-3: 2009).

Table 2. Clinker raw mix proportions, concentrations of main deleterious elements (%) and manufacturing parameters

Component	Control	APCR(5%)	APCR(15%)	APCR(35%)	w-APCR(5%)	w-APCR(15%)	w-APCR(34%)
APCR	0	5	15	35	0	0	0
w-APCR	0	0	0	0	5	15	34
$CaCO_3$	78.73	74.6	66.5	50.67	74.9	67.45	53.44
SiO_2	15.18	14.8	13.9	12.63	14.63	13.5	11.6
Al_2O_3	3.81	3.4	2.6	0.4	3.32	2.25	0.01
Fe_2O_3	2.28	2.2	2	1.3	2.15	1.8	0.95
Na as Na_2O	0	0.16	0.48	1.12	0.09	0.29	0.65
K as K_2O	0	0.13	0.38	0.88	0.04	0.13	0.30
Cl	0	0.34	1	2.52	0.03	0.08	0.17
S as SO_3	0	0.15	0.45	1.04	0.29	0.86	1.93
Zn	0	0.015	0.044	0.1	0.019	0.057	0.13
Pb	0	0.0027	0.0082	0.019	0.0035	0.01	0.024
LSF	0.91	0.91	0.92	0.93	0.91	0.92	0.94
SM	2.49	2.48	2.44	2.86	2.47	2.50	2.78
AM	1.67	1.65	1.65	1.60	1.65	1.62	1.62
HM	2.07	2.07	2.08	2.16	2.08	2.11	2.18

Lime saturation factor, LSF = $CaO/(2.8xSiO_2 + 1.2xAl_2O_3 + 0.65xFe_2O_3)$
Silica modulus, SM = $SiO_2/(Al_2O_3 + Fe_2O_3)$
Alumina modulus, AM = Al_2O_3/Fe_2O_3
Hydration modulus, HM = $CaO/(SiO_2 + Al_2O_3 + Fe_2O_3)$

Analysis of Clinkers. Simultaneous thermal analysis (STA) using a NETZSCH STA 449 C was used to investigate mass changes (thermogravimetry, TG; differential TG, DTG) and energy flows (differential scanning calorimetry, DSC) as a function of temperature, when the raw mixes were heated. A single run was conducted for each raw mix using about 200 mg of sample in an 85 μL alumina crucible (and an identical reference crucible) with a nitrogen purge gas flow rate of 100 mL/min, equilibration at 40°C for 10 min, followed by a heating rate of 10°C/min up to 1450°C and maintenance of this temperature for 30 min.

X-ray powder diffraction (XRD) was used to characterize the crystalline phases present in the clinkers. Each sample was side-loaded against a ground-glass surface into a glass-backed aluminium-framed sample holder. Diffraction patterns were measured in Bragg–Brentano reflection geometry using a Bruker D8 advance. This diffractometer is equipped with a Cu anode X-ray tube (run at 40 kV, 250 mA) and an incident beam Ni monochromator, which produces a single CuKa1 line, leading to very sharp diffraction maxima. All patterns were scanned with a step length of 0.02° and scan speed of 8°/min. Phase identification was made by search matching to the International Centre for Diffraction Data (ICDD) database using the PANanalytical proprietary software (‘‘X’Pert HighScore Plus’’). Phases were identified on the basis of a minimum of 3 diffraction lines. An internal standard (α-Al_2O_3) was used for quantitative analysis using Rietveld refinement.

The morphologies of the clinker minerals were observed using a Carl Zeiss 37081 optical microscope. The samples were cross-sectioned and polished, and the surface of the cross-section was etched by nitric acid in alcohol (1.5 mL of HNO_3 in 100 mL of C_2H_5OH) for 6-10 seconds.

Total element compositions of the raw mixes and clinkers were determined by XRF. Incorporation of elements into the mineral phases was investigated on a JEOL JSM-6480LV high-performance, variable pressure analytical scanning electron microscope (SEM) with secondary electron imaging (SEI) and backscattered electron imaging (BEI) detectors. Polished samples were mounted rigidly on a specimen stub and coated with an ultrathin layer of Au. Energy-dispersive X-ray spectroscopy (Oxford Instrument INCAx-sight EDS-system) was used for microanalysis of the solid phases viewed by SEM. SEM/EDS analysis were performed with a 15 kV accelerating voltage. About 100 spot-analyses were performed. Certified standards were used for calibration. Element detection limits were reduced to about 0.1-0.05 mass % by using long counting times. Element peaks were automatically identified in the EDS spectrum using AutoID, which also provided tools for manual validation of the elements detected. Summation of the determined elemental compositions to 100% was verified.

RESULTS AND DISCUSSION

Simultaneous Thermal Analysis of Mixtures. The TG, DTG, and DSC curves for heating of control mixes and the raw mixes containing different amounts of APCR and w-APCR are shown in Figure 1. These STA results demonstrate characteristic regions for cement clinkering in the studied interval from 25 to 1450°C and can help to understand the effects of raw and washed APCR on decomposition, crystallisation and melting behaviours during co-processing (Jackson, 1998). Changes in heat flow cannot be used for quantitative analysis because the DSC curve is based on the initial sample mass, and has an unstable base line due to the complex nature of the sample, with multiple changes in mass and heat capacity occurring as the temperature increases.

For all of the mixes, a small mass loss peak in the DTG curve (in the context of a gradual 2-3% mass increase to ~650°C, possibly due to oxidation or carbonation of sample impurities, e.g., Fe^{2+} or CaO) and an associated endothermic peak in the DSC curve, can be observed at around 100°C. These peaks become more pronounced and shift to a lower temperature with an increase in the proportion of APCR or w-APCR. It is postulated that this endotherm is mainly due to the loss of hygroscopic and chemically combined water from alkali and alkali-earth salts, including NaCl, $CaCl_2$, portlandite, gypsum and ettringite, which are present in the APCR but minimal in the reagent grade raw materials (Bogush et al. 2015 and 2019).

For all of the mixes, a small mass loss peak in the DTG curve (in the context of a gradual 2-3% mass increase to ~650°C, possibly due to oxidation or carbonation of sample impurities, e.g., Fe^{2+} or CaO) and an associated endothermic peak in the DSC curve, can be observed at around 100°C. These peaks become more pronounced and shift to a lower temperature with an increase in the proportion of APCR or w-APCR. It is postulated that this endotherm is mainly due to the loss of hygroscopic and chemically combined water from alkali and alkali-earth salts, including NaCl, $CaCl_2$, portlandite, gypsum and ettringite, which are present in the APCR but minimal in the reagent grade raw materials (Bogush et al., 2015 and 2019).

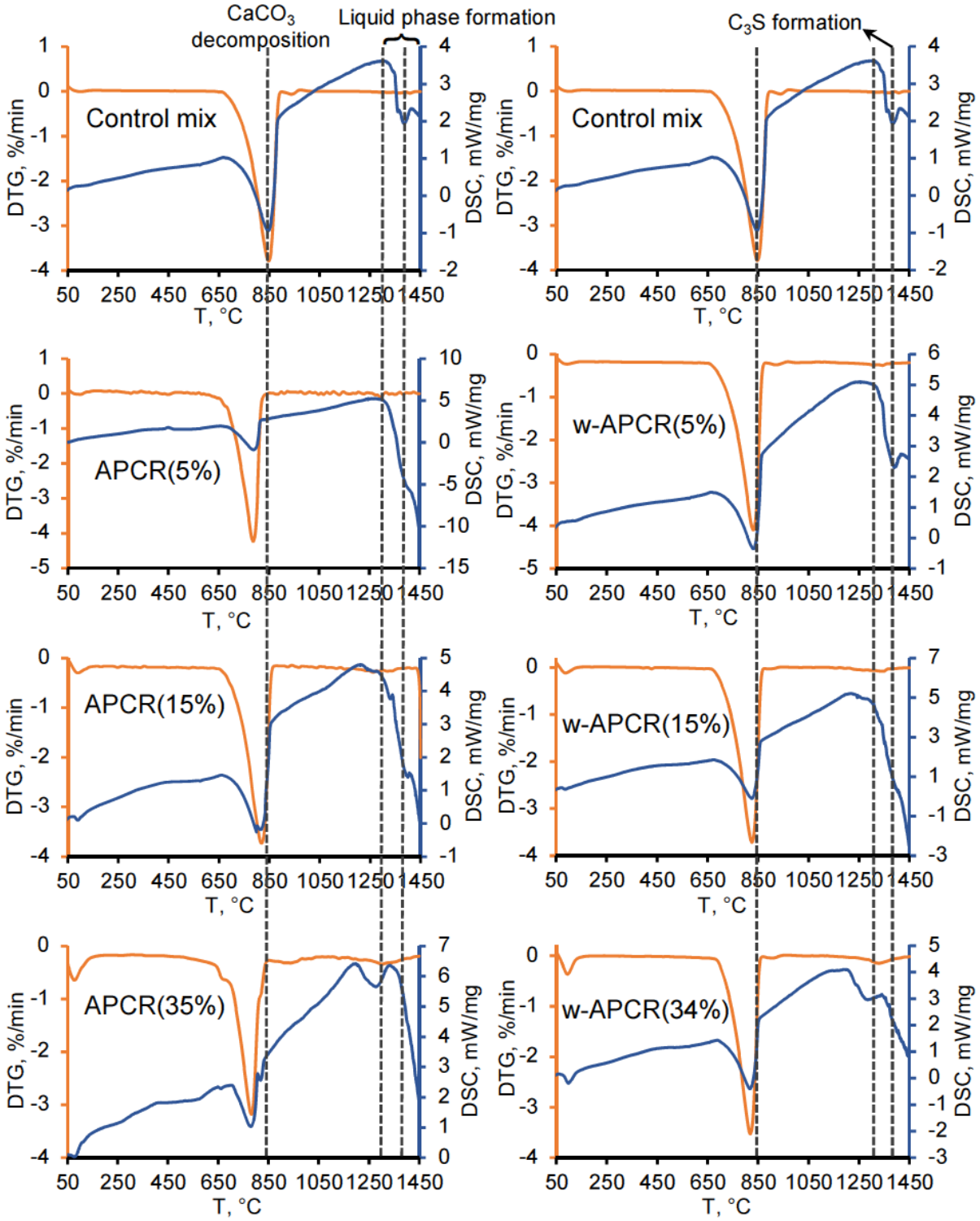

Figure 1. Differential thermogravimetry (DTG), and differential scanning calorimetry (DSC) curves of control and co-processed clinkers containing raw and washed air pollution control residues (APCR, w-APCR)**.**

Table 3. CO_2 released by thermal decomposition of $CaCO_3$

Clinker raw mix	CO_2 release (% of total mass)	
	Calculated	Measured
Control	35	34
APCR (5%)	33	32
APCR (15%)	31	31
APCR (35%)	26	23
w-APCR (5%)	34	33
w-APCR (15%)	32	31
w-APCR (34%)	28	29

A substantial mass loss, attributable mainly to release of CO_2 by the decomposition of $CaCO_3$, can be observed in the TG curve from ~650-900°C. The amounts of carbon dioxide released in this temperature range are estimated in Table 3, and accord well with theoretical releases calculated based on the compositions of the materials in the raw mixes , i.e., the chemical formulae of the analytical grade raw materials, and TG data for 100% APCR and w-APCR from Bogush et al. 2019). Addition of APCR or w-APCR decreases CO_2 release from this thermal decomposition by up to 32% and 16% (i.e., calculated in comparison to the control), respectively, because these wastes contain Ca-bearing phases other than $CaCO_3$. The associated endothermic DSC peak again shifts to a lower temperature with an increase in the proportion of APCR or w-APCR, and becomes more complex. For the highest APCR content of 35%, DTG shows a small early decomposition peak at~660°C, which is not clearly associated with an energy change. It may indicate sudden delayed degassing of the sample after the gradual decomposition of the complex phases of the APCR, e.g., CaOHCl, which decomposes at 550°C (Bogush et al. 2015). A small right-side shoulder DTG peak in clinker APCR(35%) is associated with a second overlapping endotherm at ~850^{o}C in the DSC curve. This second endotherm is also visible for clinker APCR(15%), but is notably absent for all the w-APCR clinkers,

indicating a link to the presence of soluble salts. KCl and NaCl also melt in the temperature range attributed to $CaCO_3$ decomposition (at 771°C and 801°C, respectively; Dean 1972), which likely contributes to this endothermic region in the DSC, though several distinct peaks are not recognisable.

From ~700°C, $CaCO_3$ also begins to react with silica, alumina and iron oxide; an exothermic band in the DSC curve from ~900-1250°C without mass loss corresponds to the continued solid-state reaction to form C_2S, C_3A and C_4AF (Jackson 1998). In a pure system, the liquid phase that accelerates C_3S formation and sintering is not expected to form below 1338°C (an invariant point; Telschow et al. 2012). Melting of the control sample is indicated by an endothermic region from ~1300°C. Initiation of the solid-state reactions, and then melting, shifts to lower temperatures with increased addition of APCR containing chlorides, sulphates, alkalis, and other components that can act as fluxes or/and mineralizers (Ramachandran et al. 2003). A broad, shallow mass loss peak centered at ~1300^{o}C is discernible in the DTG curves, indicating decomposition or degassing. A pronounced peak in this region for the highest waste additions can be attributed to the formation of large amount of C_2S.

In the DSC curve for the control sample, an exotherm, likely associated with crystallisation of C_3S from the melt, can be observed at ~1420^{o}C, and the curve for the w-APCR(5%) clinker appears very similar. For all of the APCR clinkers and the 15% and 34% w-APCR clinkers, a continuing negative slope of the DSC curve to the end of the test at 1450°C indicates continued uncontrolled melting due to the previously noted presence of fluxes; this is an undesirable phenomenon from the perspective of forming the desired clinker nodules, and may also affect the kiln refractory lining. Reaction peaks in this region for C_3S formation could not be clearly identified for the clinker mixes containing APCR, or the higher additions of w-APCR. A

shoulder peak at ~1420°C in the DSC curves for the clinkers with lower waste additions could still be C_3S formation, but the DSC curve becomes more complex after ~1200°C for the higher additions of both APCR and w-APCR, due to a mixture of endothermic and exothermic phenomena. Disappearance of the exotherm peak at ~1420°C in the DSC curve for APCR(35%) suggests that no C_3S is formed.

XRD Analysis. Table 4 shows the main crystalline mineral phases calculated using the Bogue method and determined by XRD-Rietveld analysis in the clinkers; the XRD test reports are provided in Appendix A. The low free lime contents (<0.2%) of all the clinkers indicate high burnability, i.e., high reactivity, of the investigated mixes. The XRD-Rietveld data shows the formation of all the usual mineral phases present in ordinary Portland cement clinker in the control and all co-processed clinkers. The two main monoclinic polymorphs of C_3S, M1 and M3, were identified in all of the clinkers, as well as the β monoclinic polymorph of C_2S. C_3A presents in both cubic and orthorhombic forms. Trace amounts of other minerals (portlandite, $Ca(OH)_2$; quartz, SiO_2; periclase, MgO; and arcanite, K_2SO_4) were identified in some clinkers.

The phase composition determined by XRD for the control clinker is comparable to the calculated Bogue composition. There are some changes in the mineral composition of the clinkers made with APCR and w-APCR. The proportion of C_3S and C_3A decreased, and the proportion of C_2S increased, with increasing addition of either APCR. The amount of C_4AF was slightly higher in clinker w-APCR(34%), probably because of the presence of Zn, as shown by others (Odler and Schmidt 1980; Stephan et al. 1999; Saikia et al. 2007).

Table 4. Main crystalline mineral phases in clinkers made with raw and washed air pollution control residues, calculated using the Bogue method (labelled, bold) and measured by X-ray diffraction (XRD) with Rietveld analysis

Clinker	**$3CaO \cdot SiO_2$ C_3S [Bogue]**	$3CaO \cdot SiO_2$ C_3S (M1) [XRD]	$3CaO \cdot SiO_2$ C_3S (M3) [XRD]	**$2CaO \cdot SiO_2$ C_2S [Bogue]**	$2CaO \cdot SiO_2$ C_2S beta [XRD]	**$3CaO \cdot Al_2O_3$ C_3A [Bogue]**	$3CaO \cdot Al_2O_3$ C_3A cubic [XRD]	$3CaO \cdot Al_2O_3$ C_3A orthorhombic [XRD]	**$4CaO \cdot Al_2O_3 \cdot Fe_2O_3$ C_4AF [Bogue]**	$4CaO \cdot Al_2O_3 \cdot Fe_2O_3$ C_4AF [XRD]	CaO Lime [XRD]	$Ca(OH)_2$ Portlandite [XRD]	SiO_2 Quartz [XRD]	MgO Periclase [XRD]	K_2SO_4 Arcanite [XRD]	Amorphous [XRD]
Control	**60.8**	41	19	**19.6**	22	**9.0**	6.9	0.48	**10.6**	9.5	0.1	0.23	0.15	-	-	0.27
APCR(5%)	**59.3**	34	15	**20.3**	38	**9.0**	3.0	1.0	**10.7**	8.5	0.03	0.43	0.18	0.07	-	0
APCR(15%)	**58.4**	19	10	**19.5**	58	**9.0**	2.2	0.6	**10.6**	8.4	-	0.39	0.03	-	-	0.96
APCR(35%)	**58.6**	1.2	4.1	**18.8**	71	**7.6**	-	1.4	**9.12**	4.7	-	-	-	1.03	0.57	15
w-APCR(5%)	**59.4**	38	14	**20.0**	30	**8.9**	5.2	0.79	**10.7**	10	0.14	0.38	0.53	-	-	0.31
w-APCR(15%)	**58.9**	31	9.7	**19.0**	44	**8.7**	2.8	1.5	**10.5**	9.4	0.16	0.39	0.48	-	-	0.67
w-APCR(34%)	**58.3**	21	1.3	**18.2**	62	**8.0**	1.4	1.2	**9.28**	11	0.12	0.24	-	0.39	0.11	0.52

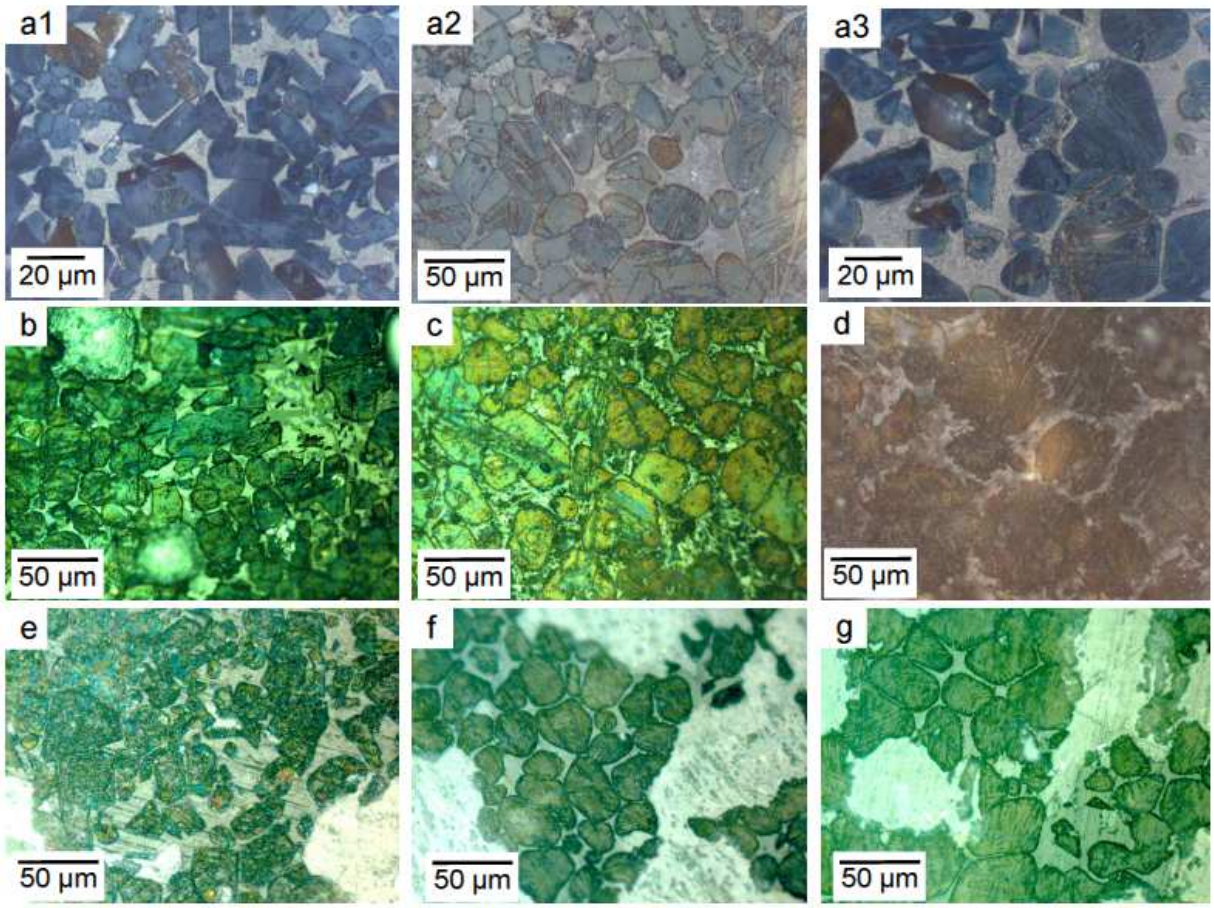

Figure 2. Light microscopy photographs of the cement clinkers: a1, a2, a3 – control clinker; b – APCR (5%) clinker; c – APCR (15%) clinker; d – APCR (35%) clinker; e – w-APCR (5%) clinker; f – w-APCR (15%) clinker; g – w-APCR (34%) clinker.

Light Microscopy Analysis. Light microscopy of the clinkers showed angular, hexagonal crystals, typical of C_3S, and round crystals with multidirectional lamellae, typical of C_2S. Dark and bright interstitial phases are typical of C_3A, and C_4AF, respectively (Figure 2) (Taylor 1997). The amount and size of the C_2S crystals can be observed to increase with addition of either APCR, particularly in the clinker with 35% APCR. The crystals of C_3S and C_2S in the control clinker have well-defined geometric shapes (Figure 2), but addition of 15 and 35% of APCR resulted in poor crystallization, with prominent lamellar extensions from the C_2S crystals into the

interstitial matrix. Diffuse boundaries between the phases are also an indicator of poor crystallization.

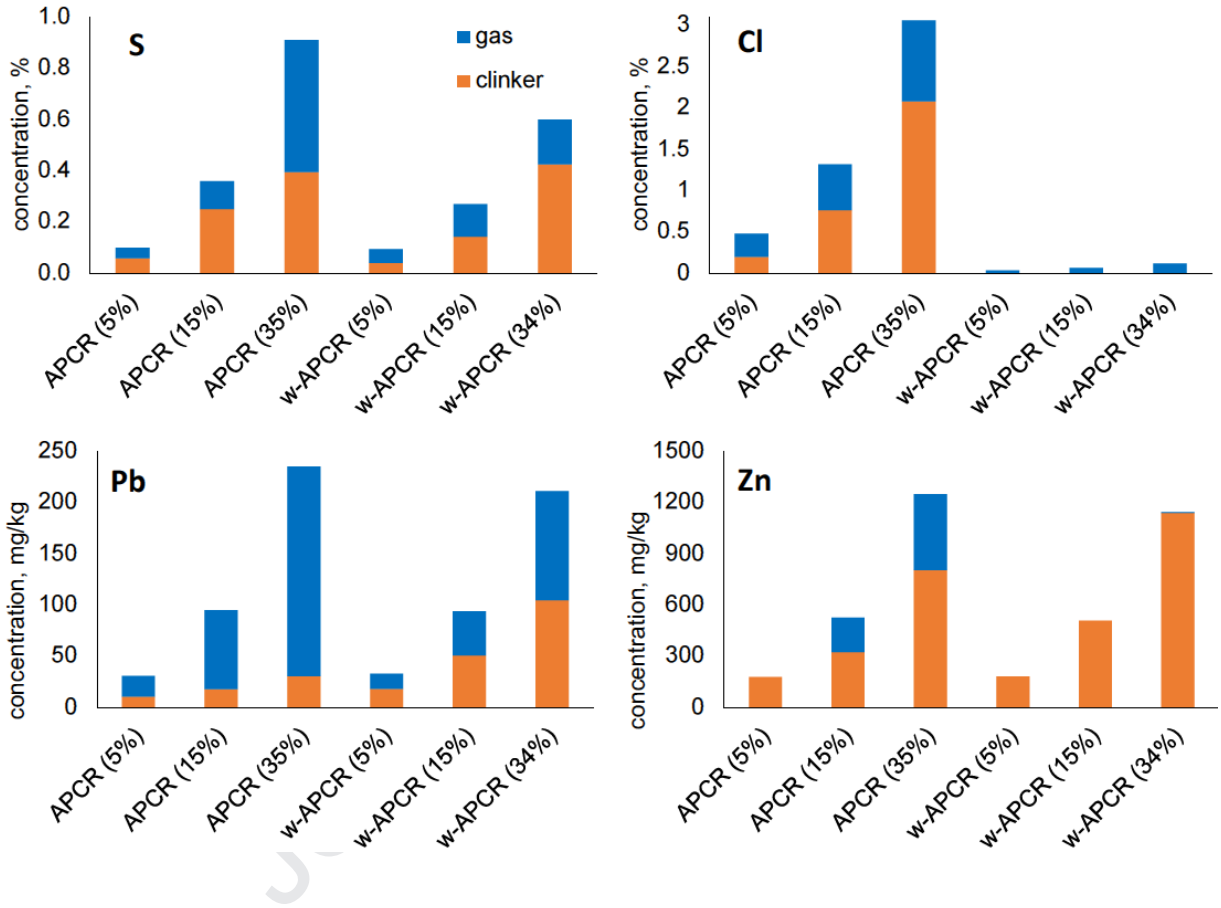

Figure 3. Distribution of S, Cl, Pb and Zn concentrations between the gas and clinker (expressed as concentration volatilised from, or remaining in, the clinker, respectively).

Element Volatilization Ratios. Mass balance calculations based on the mass loss measured by TG, and the elemental compositions of the raw mixes and clinker, showed that Al, Si, Ca, Mg, Fe, Ti, and Cr were fully incorporated in the clinkers. Figure 3 shows the measured concentrations of S, Cl, Pb and Zn in the clinkers, and the calculated quantities emitted in the gas, expressed as concentrations lost from the clinkers. Volatilisation of both S and Cl was high

and increased with addition of the APCR and w-APCR, but washing decreased both the amount and proportion of volatilised S, and the amount of Cl available for volatilisation.

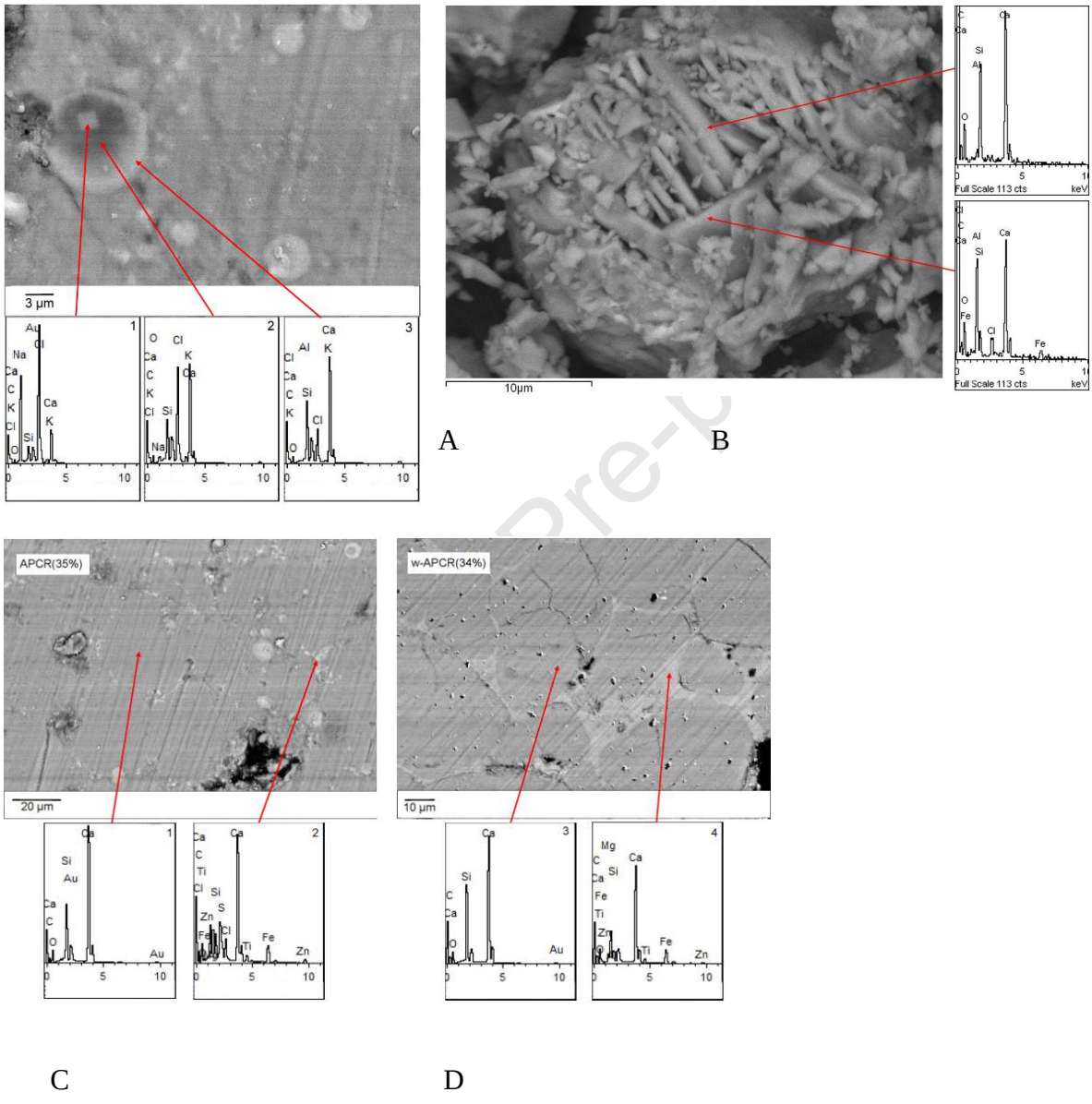

Figure 4. Scanning electron microscopy image with energy dispersive x-ray spectroscopy of clinker APCR(35%), showing bubble capture of halite and incorporation of Cl (A); C2S showing incorporation of Cl in clinker APCR(35%) (B) ; polished APCR (C) and w-APCR (D) clinker showing incorporation of Zn in interstitial phases.

A significant amount of Cl was incorporated in the clinker made with APCR, and the final concentration (of up to 2%) exceeded the level of 0.1% by mass permitted in Portland cement

(BS EN 197-1: 2011). Excessive chloride can have detrimental effects on cement paste properties, including acceleration of setting, and matrix disruption at later ages due to formation of Friedel's salt, as well as causing corrosion of steel reinforcement in cement products. As shown by the STA, the chlorine, sulphur and alkalis introduced with the APCR increased the formation of liquid and gas phases, which appears to have resulted in capture of bubbles in the liquid phase. Upon cooling, the gases in the bubbles condensed, forming halite. Cubic crystals of NaCl (halite) were observed in gas bubbles captured in clinker APCR(35%) (Figure 4A). Also, SEM/EDS showed that Cl can be incorporated in C_3S and C_2S (Figure 4B and Table 5a). In any case, the chloride content of clinkers made with w-APCR is less than 2 mg/kg.

Figure 3 also shows that a large proportion of Pb was volatilised in co-processing of APCR, with the emitted proportion increasing from 65% from clinker APCR(5%) to 87% from clinker APCR(35%). However, washing the APCR reduced Pb volatilisation by ~50%. Volatilisation of Zn in co-processing also increased with addition of APCR, but was eliminated by washing of the APCR. Since the total clinker concentrations of Pb and Zn were only marginally decreased by washing (Bogush et al. 2013 and 2019), their decreased volatilisation after washing is attributable to the removal of other species, notably chloride, in the washing process. In previous work, Pb was found to be speciated mainly as Pb-glass, with some $PbSO_4$, and small amounts of PbO and $PbCl_2$, in both the APCR, and w-APCR (Bogush et al. 2019), whereas $Zn_5(CO_3)_2(OH)_6$ and $ZnFe_2O_4$ and $Zn_4Si_20_7(OH)_2 \cdot H_2O$ appeared to be the most likely forms of Zn in both residues (Bogush et al. 2013), with only minor changes in speciation resulting from washing. Decreased Pb and Zn volatilisation as a result of washing must therefore be attributed mainly to the influence of salts on melting behaviour, and element volatility, decreasing, for example, the

melting points of 886°C and 1975°C, and boiling points of 1472°C and 2360°C for pure PbO and ZnO (Dean 1972), respectively.

These results are consistent with previous findings in the literature (Saikia et al. 2007, Wang et al. 2010). It must be noted that these phenomena were observed in a laboratory kiln; it is not known whether they would occur at full scale. In a commercial dry process rotary cement kiln, air addition is controlled, and gas flow is usually counter-current to the raw materials, through the calciner, pre-heater, and, often, the raw mill, which provides additional opportunities for the gaseous elements, such as chlorine, to interact with the solids. Since circulating chloride can lead to formation of low melting point mixture that lead to preheater blockages (Jackson 1998), a by-pass is usually operated to purge excess chlorine from the system, which necessary also purges other volatile species. Yan et. (2018) reported on a full-scale trial in which most Pb and Zn were captured in clinker, but the APCR addition investigated was sufficiently low that the main sources of these elements were conventional raw materials and coal.

Zn incorporation in clinker phases. The concentration of Pb in the clinkers was too low to examine by EDS, but Table 5 summarises the spot analyses for the calcium silicate (a) and interstitial (b) phases in clinkers APCR(35%) and w-APCR(34%), which were targeted based on their morphologies. While these EDS spot analyses provide information about the composition of these phases, they are not fully representative of the whole sample, due to their small size; nevertheless, the mean and ranges in Table 5 are notable for their consistency. C_3S and C_2S showed no incorporation of Zn. Zn was found mainly in the interstitial phases (Figure 4C and D), where the fineness and intergrowth of C_3A and C_4AF hindered accurate targeting of either of these phases for spot analyses. Solid solution by isomorphous replacement of Al^{3+} or Fe^{3+} (Al^{3+} - ionic radius 0.39-0.54 and electronegativity 1.61; Fe^{3+} - 0.63-0.92 and 1.83) by Zn^{2+} (0.6-0.9 and

1.65) is probable. The stoichiometric proportions in Table 5b) are consistent with substitution of Zn^{2+} for Al^{3+} or Fe^{3+} in C_4AF, if it is assumed that Mg likewise substitutes for Al/Fe (Taylor 1997); on the other hand, substitution of Zn^{2+} for Al^{3+} in C_3A is possible, if it is assumed that Mg^{2+} substitutes for Ca^{2+} in C_3A. Uptake of other elements in this way is known to be typical of both C_3A and C_4AF in Portland cement (Taylor 1997). Since both C_3A (especially) and C_4AF will hydrate when the clinker is hydrated, the potential for release of Zn and other incorporated elements from the hydrated paste must be considered.

Table 5a. Composition of calcium silicate phases estimated by scanning electron microscopy with energy dispersive X-ray spectroscopy (moles)

		35% APCR		34% w-APCR	
	C_3S	Average	Range (n=5)	Average	Range (n=17)
Na		0.015	0 - 0.038	0.0025	0 - 0.013
Ca	0.60	0.58	0.52 - 0.61	0.60	0.55 - 0.62
Mg		0.013	0 - 0.042	0.013	0.004 - 0.024
Si	0.20	0.21	0.18 - 0.22	0.19	0.17 - 0.23
Al		0.036	0.001 - 0.066	0.012	0.008 - 0.016
Fe		0.025	0.009 - 0.036	0.002	0 - 0.01
Ti		0.005	0 - 0.023	0.004	0 - 0.019
O	1.00	1.00	1.00 - 1.00	1.00	1.00 - 1.00
Cl		0.047	0.01 - 0.071		-
S		0.011	0.008 - 0.014		-
	C_2S	Average	Range (n=12)	Average	Range (n=10)
Na				0.002	0 - 0.009
Ca	0.50	0.50	0.46 - 0.55	0.50	0.46 - 0.54
Mg		0.004	0 - 0.025	0.006	0 - 0.012
Si	0.25	0.23	0.18 - 0.26	0.2	0.16 - 0.25
Al		0.01	0 - 0.026	0.025	0.011 - 0.057
Fe			-	0.01	0 - 0.04
Ti			-	0.002	0 - 0.009
O	1.00	1.00	1.00 -	1.00	1.00 - 1.00
Cl		0.007	0 - 0.059		-
S		0.002	0 - 0.003		-

Table 5b. Composition of calcium aluminate and ferrite phases estimated by scanning electron microscopy with energy dispersive X-ray spectroscopy (moles)

			35% APCR (n=7)		34% w-APCR (n=18)	
	C_3A	C_4AF	Average	Range	Average	Range
Ca	0.50	0.40	0.47	0.40 - 0.61	0.43	0.39 - 0.51
Mg			0.02	0.01 - 0.04	0.05	0.03 - 0.06
Al	0.33	0.20	0.13	0.05 - 0.22	0.16	0.10 - 0.21
Fe		0.20	0.07	0.03 - 0.11	0.11	0.06 - 0.14
Si			0.11	0.06 - 0.18	0.05	0.02 - 0.10
Ti			0.01	0.00 - 0.02	0.02	0.00 - 0.02
Zn			0.01	0.00 - 0.02	0.01	0.00 - 0.01
Al+Fe+Si+Ti+Zn	0.33	0.40	0.34		0.35	
O	1.00	1.00	1.00	1.00 - 1.00	1.00	1.00 - 1.00
Cl			0.07	0.04 - 0.09	0.00	0.00 - 0.00
S			0.01	0.00 - 0.06	0.00	0.00 - 0.01

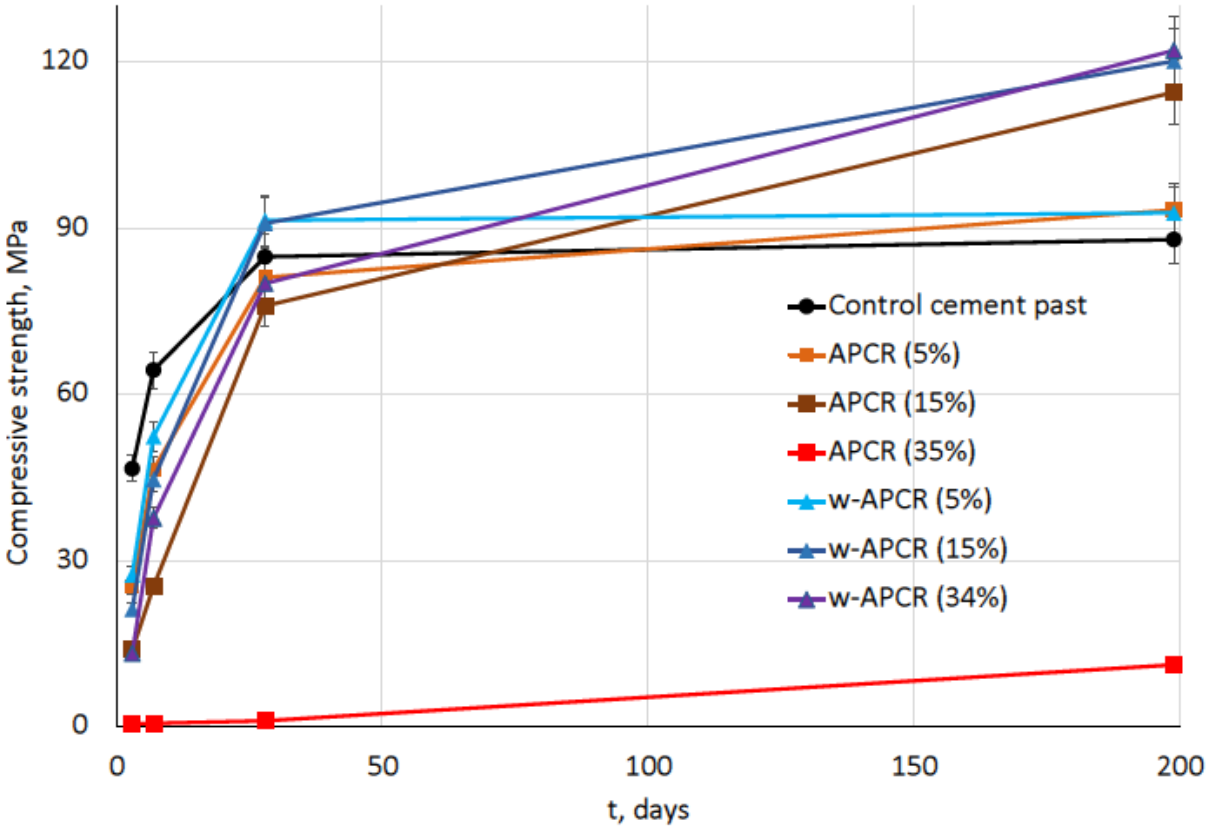

Figure 5. Unconfined compressive strength of control cement pastes and co-processed cement pastes containing raw (APCR) or washed (w-APCR) air pollution control residues.

Unconfined Compressive Strength of Co-processed Cement Pastes. The unconfined compressive strength values for cement pastes prepared with the control and all co-processed clinkers containing APCR or w-APCR at 3, 7, 28 and 199 days are shown in Figure 5. As is typical for Portland cement, the strength of the control cement paste increased gradually during the first 28 days and then remained constant. The co-processed cement pastes all showed delayed strength development during the first 7 days of curing, which was likely due to their reduced contents of the C_3S that is responsible for hardening at early ages; a monotonic relationship between strength and APCR content was not as apparent as in other work (e.g., Ma et al. 2004).

The pastes made with clinkers containing only 5% of the wastes then showed a similar strength (~90 MPa) to the control from 28d. The strengths of the cement pastes prepared with clinkers containing higher waste additions, APCR(15%), w-APCR(15%), and w-APCR(34%) were also similar to the control at 28d, but then increased significantly up to ~120 MPa at 6m. The higher proportion of C_2S, also observed by previous workers (see Introduction) is responsible for this higher and later strength development. Washing the APCR did not clearly improve strength development, except at the highest addition; the cement paste made with clinker APCR(35%) had very low compressive strength at all ages, achieving a maximum of only 13 MPa after 199 days curing. The observed damaged C_2S phase appeared to be unable to react to produce the calcium silicate hydrate responsible for strength, even at later ages.

CONCLUSIONS

Clinker reactions in co-processing of balanced raw mixes containing raw and washed APCR were noticeably affected, with the exception of that containing 5% washed APCR. The resulting clinkers contained the mineral phases typical of ordinary Portland cement clinker with only a trace of free lime, but with increased formation of C_2S and decreased formation of C_3S and C_3A, as observed by other authors. Cement paste prepared with the clinker containing the highest raw APCR addition (35%) exhibited negligible strength after 28d. Cement pastes prepared with the other co-processed clinkers had strengths that were lower than that of the control at 7d, similar at 28d (~90 MPa) and higher at 6m (up to 120 MPa), consistent with their C_2S contents. Cements with low early strength may be acceptable in some applications, but there is a trade-off between beneficial utilization of the Ca, Al and Si in APCR and detrimental effects on the manufacturing process and product quality caused by the alkalis, Cl, S, and metals in raw and washed, if any

significant quantity is co-processed. The life cycle impacts of APCR washing, which uses water and produces contaminated salty wastewater, and are an additional concern.

Volatilization of S, Cl, Pb and Zn during co-processing of raw APCR was significant, but could be reduced by washing, which fully eliminated volatilization of Zn. In the clinker, Zn was found mainly in the interstitial phases; examination of the stoichiometric composition of these phases suggests that Zn^{2+} may substitute for Al^{3+} or Fe^{3+} in C_4AF, or for Al^{3+} in C_3A. Since cement is distributed throughout the built environment, further investigation is required to determine whether Zn and other incorporated elements may be released from the cement paste when these phases react with water.

It was demonstrated that APCR co-processing may reduce CO_2 emissions by avoiding $CaCO_3$ decomposition, but it would arguably be more straight-forward to conserve CO_2 emissions by optimizing the amount of lime added in air pollution control systems. In any case, lime contents of APCR are sufficiently variable that the impact of APCR co-processing on emissions reductions is uncertain.

ACKNOWLEDGMENTS

The authors gratefully acknowledge the valuable assistance of Jim Davy in UCL Earth Sciences with the SEM/EDS, Steven Firth from UCL Chemistry with STA, and staff of the China Resources Cement Technology R&D Center, Guangzhou, with the XRD. This work was conducted with funding from the UK Engineering and Physical Sciences Research Council (Grant EP/M00337X/1) and the National Science Foundation of China (Grant No. 51461135006).

REFERENCES

Achternbosch, M., Bräutigam, K.-R., Hartlieb, N., Kupsch, C., Richers, U., Stemmermann P., 2005. Impact of the use of waste on trace element concentrations in cement and concrete. Waste Management & Research 23, 328–337.

Amutha Rani, D., Boccacchini, A.R., Deegan, D., Cheeseman, C.R., 2008. Air pollution control residues from waste incineration: current UK situation and assessment of alternative technologies. Waste Management 28(11), 2279–2292.

Astrup, T., 2008. Management of APC Residues from W-t-E Plants: An Overview of Management Options and Treatment Methods; ISWA-WG Thermal Treatment of Waste, Subgroup APC Residues from W-t-E plants, second edition, Technical University of Denmark, Denmark.

Bogush, A.A., Stegemann, J.A., 2013. Zinc Speciation in Air Pollution Control Residues from UK Energy-from Waste Facilities, Report for the Environment Agency, Centre for Resource Efficiency & the Environment, Department of Civil, Environmental & Geomatic Engineering (CEGE), University College London.

Bogush, A.A., Stegemann, J.A., Roy A., 2015. Element composition and mineralogical characterisation of air pollution control residue from UK energy-from-waste facilities. Waste Management 36, 119-129.

Bogush, A.A., Stegemann, J.A., Roy, A., 2019. Changes in composition and lead speciation due to water washing of air pollution control residue from municipal waste incineration. Journal of Hazardous Materials 361, 187-199.

BS EN 12390-3: 2009. Testing hardened concrete. Compressive strength of test specimens.

BS EN 197-1: 2011. Cement. Composition, specifications and conformity criteria for common cements.

Chandler, A.J., Eighmy, T.T., Hjelmar, O., Kosson, D.S., Sawell, S.E., Vehlow, J., van der Sloot, H.A., Hartlén, J. (Eds.), 1997. Municipal Solid Waste Incinerator Residues: Studies in Environmental Science, Vol. 67. Elsevier Science B.V., Amsterdam.

Dean, J.A., 1972. Lange's Handbook of Chemistry. 15th edition. McGraw-Hill, Inc., New York, USA.

Gomes, H.I., Mares, W.M., Rogerson, M., Stewart, D. I., Burke,I.T., 2016. Alkaline residues and the environment: a review of impacts, management practices and opportunities, Journal of Cleaner Production 112, 3571-3582.

Jackson, P.J., 1998. Portland Cement: Classification and Manufacture; in: P.C. Hewlett (Ed.), Lea's Chemistry of Cement and Concrete, 4th Edition, Butterworth Heineman, UK.

Karakas, F., Roy, A., Solpuker, U., Bogush, A.A., Stegemann, J.A., 2019. Arsenic speciation and pH-dependent leaching from cement paste from industrial waste co-processing, 1st International Conference on Innovation in Low-carbon Cement and Concrete Technology, London, UK.Lam, C. H. K., Barford, J. P., McKay, G., 2011. Utilization of municipal solid waste incineration ash in Portland cement clinker. Clean Technologies and Environmental Policy 13, 607-615.

Lederer, J., Bogush, A., Fellner, J., 2017a. The utilization of solid residues from municipal solid waste incineration in the cement industry: a review. 16th International Waste Management and Landfill Symposium, Sardinia, Italy.

Lederer, J., Trinkel, V. Fellner J., 2017b. Wide-scale utilization of MSWI fly ashes in cement production and its impact on heavy metal contents in cements: The case of Austria. Waste Management 60, 247-258.

Lin, K. L., Lo, K. W., Shie, J. L., Tuan, B. L. A., Hwang, C. L., Chang,Y. M., 2015. Hydration characteristics of cement for co-sintered from washed-fly ash and waste sludge. Environmental Progress & Sustainable Energy 34, 964-972.

Ma, B., Huang, X., Li, X.-g., Yu Z.-q., Ke, K., 2009. Research on sintering cement clinker by using the municipal solid waste incineration fly ash. Journal of Wuhan University of Technology 31, 51-54.

Marchand, L., Van Ewijk, S., Stegemann, J.A., 2019. Metabolism of metals from co-processing of energy-from-waste air pollution control residue in cement kilns, 5th International Conference on Sustainable Construction Materials and Technologies (SCMT5), Kingston, UK.

Nidheesh, P.V., Kumar, M.S., 2019. An overview of environmental sustainability in cement and steel production, Journal of Cleaner Production 231, 856-871.

Odler, I., Schmidt, O., 1980. Structure and properties of Portland cement clinkers doped with zinc oxide. Journal of the American Ceramic Society 63, 13–16.

Pan, J. R., Huang, C. P., Kuo J. J., Lin, S.H., 2008. Recycling MSWI bottom and fly ash as raw materials for Portland cement. Waste Management 28, 1113-1118.

Quina, M.J., Bordado, J.C., Quinta-Ferreira, R.M., 2008. Treatment and use of air pollution control residues from MSW incineration: an overview. Waste Management 28(11), 2097–2121.

Quina, M.J., Bordado, J.M., Quinta-Ferreira, R.M., 2014. Recycling of air pollution control residues from municipal solid waste incineration into lightweight aggregates. Waste Management 34, 430–438.

Quina, M.J., Bontempi E., Bogush A., Schlumberger S., Weibel G., Braga R., Funari V., Hyks J., Rasmussen E., Lederer J., 2018. Technologies for the management of MSW incineration ashes from gas cleaning: new perspectives on recovery of secondary raw materials and circular

economy. Science of the Total Environment 635, 526-542.Ramachandran, V.S., Paroli, R.M., Beaudoin, J.J., Delgado, A.H., 2003. Handbook of Thermal Analysis of Construction Materials. Noyes Publications, William Andrew Publishing, Norwich, New York, USA.

Saikia N., Kato S., Kojima T., 2007. Production of cement clinker from municipal solid waste incineration (MSWI) fly ash. Waste Management 27, 1178–1189.

Shi, H., 2004. Calcination of municipal solid waste incineration fly ash as cement clinker. Cement Technology, 1-4.

Solpuker, U., Stegemann, J.A., Zhou, Q., Bogush, A.A., Zhang, W.S., Wei, J.X., 2019. Metal mobility in cement paste from co-processing of energy-from-waste air pollution control residue, Cement and Concrete Science Conference (39th CCS), Bath, UK.

Stegemann, J.A., 2014. The potential role of energy-from-waste air pollution control residues in the industrial ecology of cement. Journal of Sustainable Cement-Based Materials 3(2), 111−127.

Stegemann, J.A., Zhou, Q., Bogush, A.A., Zhang, W.S., Wei, J.X., Metabolism of toxic metals in co-processing of municipal solid waste combustion air pollution control residues in cement kilns – A critical review, unpublished.

Stephan, D., Mallmann, R., Knöfel, D., Härdtl, R., 1999. High intakes of Cr, Ni, and Zn in clinker: Part I. Influence on burning process and formation of phases, Cement and Concrete Research 29(12), 1949−1957.

Taylor, H.F.W., 1997. Cement Chemistry. Thomas Telford, London.

Telschow, S., Frandsen, F., Theisen, K., Dam-Johansen, K., 2012. Cement Formation. A Success Story in a Black Box: High Temperature Phase Formation of Portland Cement Clinker. Industrial Engineering Chemistry Research 51, 10983−11004.

Wang, L., Jin, Y. Y., Nie, Y. F., Li, R.D., 2010. Recycling of municipal solid waste incineration fly ash for ordinary Portland cement production: A real-scale test. Resources Conservation and Recycling 54, 1428-1435.

Wang, L., Niu, C., Li , R.D., 2018. Prediction of arsenic and antimony behaviour in MSWI fly ash during co-processing in a cement kiln. Waste and Biomass Valorization 9, 1475-1484.

Yan, D. H., Z. Peng, L. F. Yu, Y. Z. Sun, R. Yong & K. H. Karstensen (2018) Characterization of heavy metals and PCDD/Fs from water-washing pretreatment and a cement kiln co-processing municipal solid waste incinerator fly ash. Waste Management 76, 106-116.

WBCSD, 2014. Guidelines for Co-Processing Fuels and Raw Materials in Cement Manufacturing; Cement Sustainability Initiative (CSI), World Business Council for Sustainable Development.

Wexell, D., 2005. Vitrification of Ash from Waste-to-energy Incinerators, Part II. Cold Crown Melting and Parameters for Scale-up; Pacific Northwest Pollution Prevention Resource Center, Corning Inc., NY, USA.

Highlights

- Cement clinker was made with energy-from-waste air pollution control residue (APCR)
- APCR co-processing may reduce CO_2 emissions by avoiding $CaCO_3$ decomposition
- APCR co-processing also affects clinker minerals and cement quality
- Cl^-, SO_4^{2-} and alkalis affect kiln reactions and increase Zn and Pb in stack gas
- Zn is in solid solution in $4CaO \cdot Al_2O_3 \cdot Fe_2O_3$ or $3CaO \cdot Al_2O_3$ and could be mobile

Declaration of interests

☒ The authors declare that they have no known competing financial interests or personal relationships that could have appeared to influence the work reported in this paper.

☐~~The authors declare the following financial interests/personal relationships which may be considered as potential competing interests:~~